Multi-channel analysis of the $^{18}O + {}^{48}Ti$ reaction at 275 MeV within the NUMEN project

Giuseppe Antonio Brischetto

for the NUMEN collaboration

Istituto Nazionale di Fisica Nucleare, Laboratori Nazionali del Sud, Catania, Italy

6º Incontro Nazionale di Fisica Nucleare (INFN2024)

26 – 28 February 2024, Trento (Italy)

Neutrinoless double beta (0νββ) decay

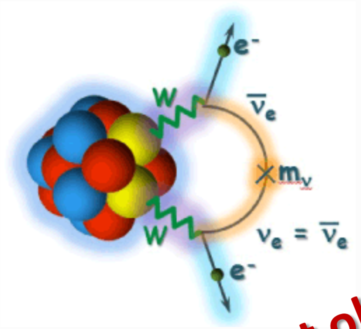

E. Majorana, Il Nuovo Cimento 14 (1937) 171
W. H. Furry, Phys. Rev. 56 (1939) 1184

$$ {}^{A}_{Z}X_{N} \rightarrow {}^{\;\;\;A}_{Z+2}Y_{N-2} + 2e^{-} $$

Not observed yet!

- **Forbidden** by the Standard Model (total leptonic number is not conserved)
- Prominent tool to establish:
  - **Neutrino nature**: Dirac or Majorana?
  - **Neutrino absolute mass** scale

$$ \left[T^{0\nu}_{1/2}\right]^{-1} = G_{0\nu} \left|M_{0\nu\beta\beta}\right|^{2} \left|f(m_i)\right|^{2} $$

Phase-space factor

Nuclear matrix element (NME)

contains the effective **neutrino mass**

Neutrinoless double beta (0νββ) decay

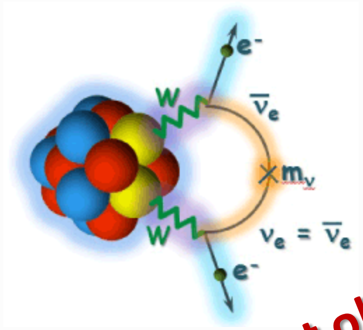

E. Majorana, Il Nuovo Cimento 14 (1937) 171
W. H. Furry, Phys. Rev. 56 (1939) 1184

$$^{A}_{Z}X_{N} \rightarrow {}^{A}_{Z+2}Y_{N-2} + 2e^{-}$$

Not observed yet!

- **Forbidden** by the Standard Model (total leptonic number is not conserved)
- Prominent tool to establish:
  - **Neutrino nature**: Dirac or Majorana?
  - **Neutrino absolute mass** scale

$$\left[T^{0\nu}_{1/2}\right]^{-1} = G_{0\nu} \left|M_{0\nu\beta\beta}\right|^{2} \left|f(m_i)\right|^{2}$$

Phase space factor

Nuclear matrix element (NME)

contains the effective **neutrino mass**

$$M_{0\nu\beta\beta} = \langle \Psi_f | \hat{O}_{0\nu\beta\beta} | \Psi_i \rangle$$

- NMEs **are not** physical observables
- The challenge is the description of the **nuclear many body states**
- **Calculations** (still sizeable uncertainties): QRPA, Large scale shell model, IBM, EDF, ab-initio …..

Accessible only through theoretical calculations

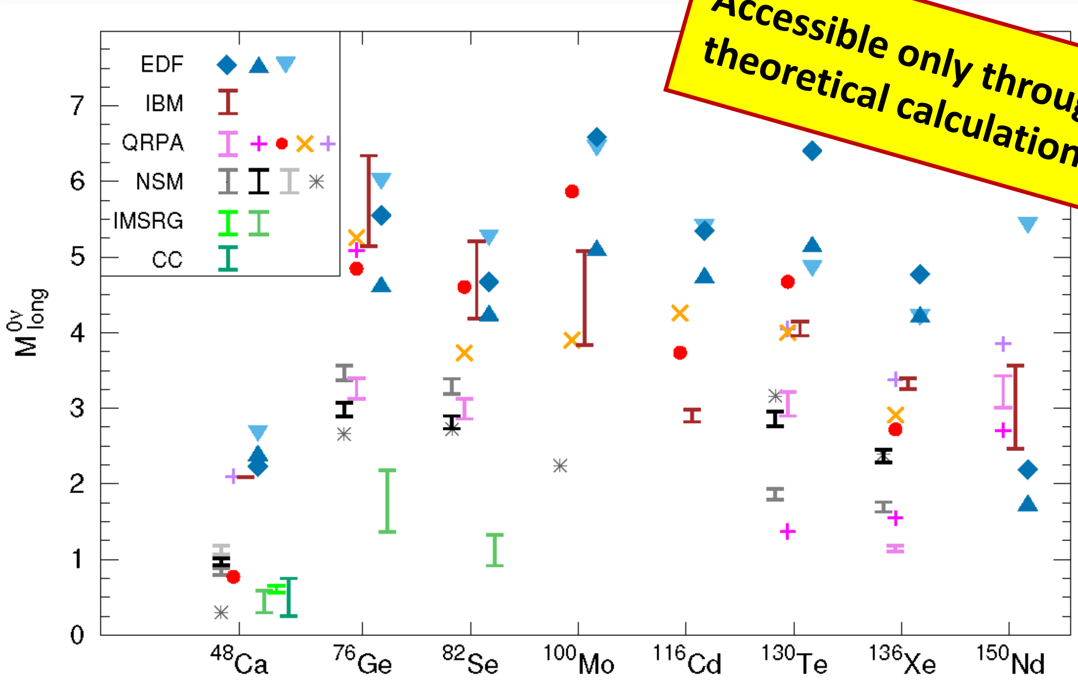

M. Agostini et al., Rev. Mod. Phys. 95 (2023) 025002
H. Ejiri et al., Phys. Rep. 797 (2019) 1–102

Neutrinoless double beta (0νββ) decay

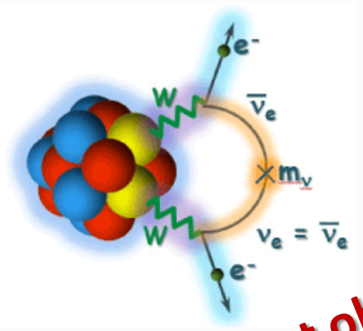

E. Majorana, Il Nuovo Cimento 14 (1937) 171
W. H. Furry, Phys. Rev. 56 (1939) 1184

$$ {}^{A}_{Z}X_{N} \rightarrow {}^{A}_{Z+2}Y_{N-2} + 2e^{-} $$

Not observed yet!

- **Forbidden** by the Standard Model (total leptonic number is not conserved)
- Prominent tool to establish:
  - **Neutrino nature**: Dirac or Majorana?
  - **Neutrino absolute mass** scale

$$ \left[T^{0\nu}_{1/2}\right]^{-1} = G_{0\nu} \left|M_{0\nu\beta\beta}\right|^{2} \left|f(m_i)\right|^{2} $$

Phase space factor

Nuclear matrix element (NME)

contains the effective **neutrino mass**

$$ M_{0\nu\beta\beta} = \langle \Psi_f | \hat{O}_{0\nu\beta\beta} | \Psi_i \rangle $$

- NMEs **are not** physical observables
- The challenge is the description of the **nuclear many body states**
- **Calculations** (still sizeable uncertainties): QRPA, Large scale shell model, IBM, EDF, ab-initio .....

Accessible only through theoretical calculations

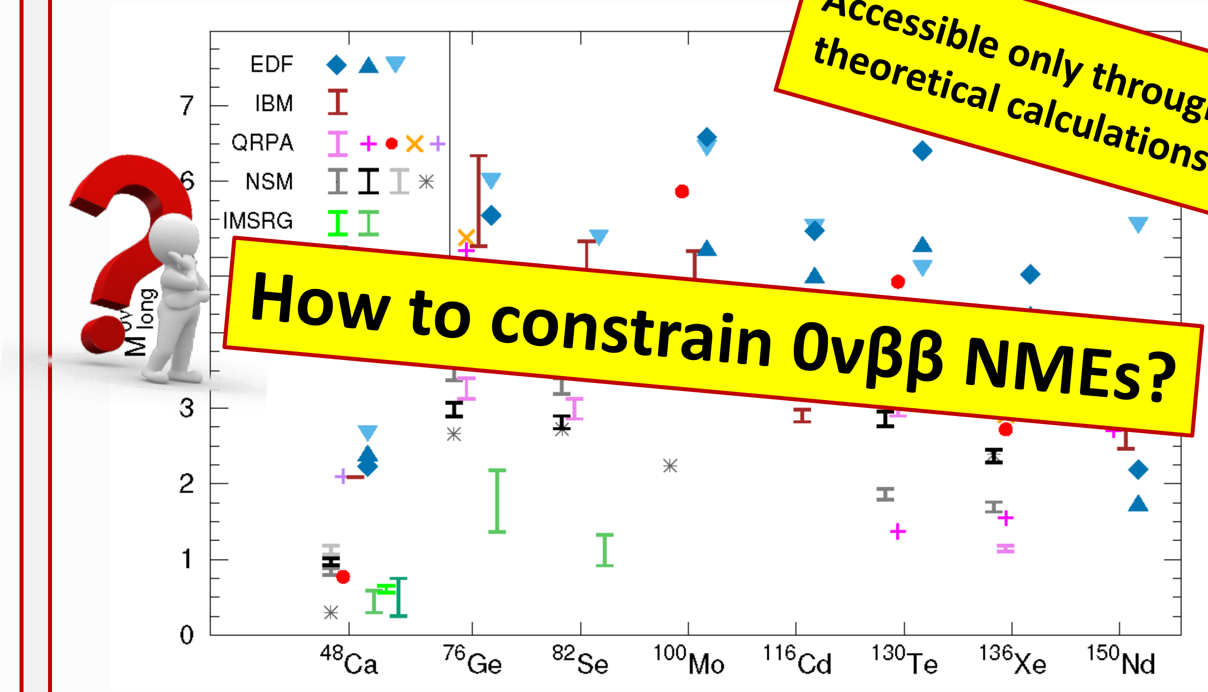

How to constrain 0νββ NMEs?

M. Agostini et al., Rev. Mod. Phys. 95 (2023) 025002
H. Ejiri et al., Phys. Rep. 797 (2019) 1–102

Experimental approaches to constrain 0νββ NMEs

Experimental probes for 0νββ NMEs:

- ✓ β-decay and **2νββ** decay
- ✓ **(π⁺, π⁻)**, single charge exchange **(³He,t)**, **(d,²He)**, **HI-SCE**, **electron capture**, transfer reactions, μ-**capture**, **γ-ray spectroscopy**, **γγ-decay**, etc.
- ✓ A promising experimental tool: **Heavy-Ion Double Charge-Exchange (HI-DCE)**

1st order isospin probes

2nd order isospin probes

DCE reaction

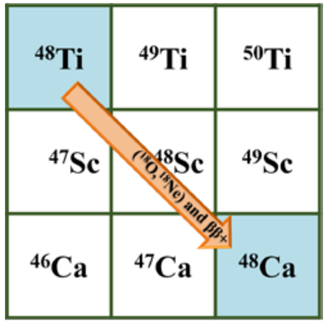

$${}^{a}_{z}x_{n} + {}^{A}_{Z}\mathrm{X}_{N} \rightarrow {}^{a}_{z-2}y_{n+2} + {}^{A}_{Z+2}\mathrm{Y}_{N-2}$$

$$M_{DCE} = \langle \Psi_f | \hat{O}_{DCE} | \Psi_i \rangle$$

NUclear
Matrix
Elements for
Neutrinoless double
beta decay

F. Cappuzzello et al., Eur. Phys. J. A 54 (2018) 72

Deduce data-driven information about the **0νββ** decay **NMEs** by using **DCE** nuclear reactions induced by **heavy ions**.

Heavy-ion DCE reaction vs. 0νββ

Differences

- DCE mediated by **strong interaction**, 0νββ by **weak interaction**
- Reaction dynamics vs. decay
- DCE includes **sequential** multinucleon transfer **mechanism**
- **Projectile and target** contributions in the NME

Similarities

- **Same initial and final states:** Parent/daughter states of the $0\nu\beta\beta$ decay are the same as those of the target/residual nuclei in the DCE
- **Similar operator:** Fermi, Gamow-Teller and rank-2 tensor components are present in both the transition operators, with tunable weight in DCE
- **Large linear momentum** (~100 MeV/c) available in the virtual intermediate channel
- **Non-local** processes: characterized by two vertices localized in a pair of nucleons
- **Same nuclear medium**
- **Off-shell propagation** through virtual intermediate channels

The NUMEN experiments @ INFN-LNS

K800 Superconducting Cyclotron

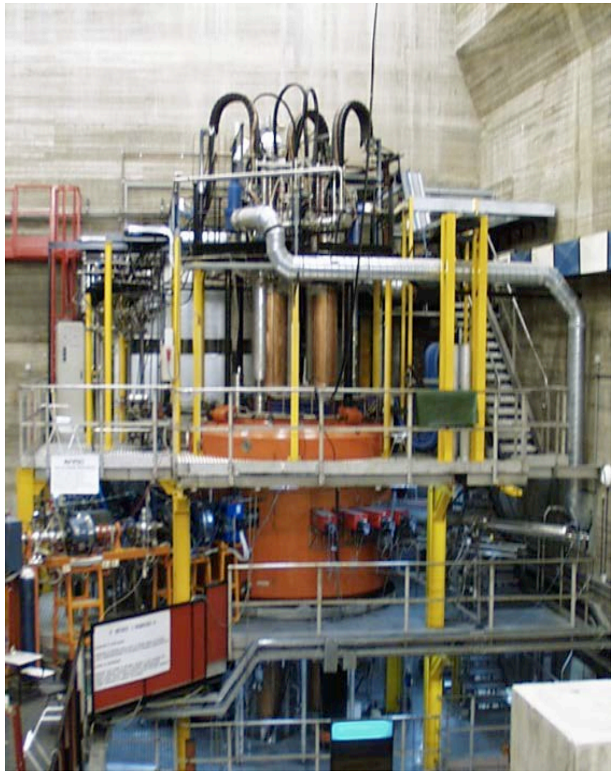

- In operation since 1996.
- Accelerates ions from H to U
- Maximum energy 80 MeV/u.

MAGNEX magnetic spectrometer

Optical characteristics	Measured values
Solid angle	50 msr
Angular range	from –20° to +85°
Momentum acceptance	-14%, +10%
Momentum dispersion	3.68 cm/%
Maximum magnetic rigidity	1.8 T m

Measured resolutions:
- Energy $\Delta E/E \sim 1/1000$
- Angle $\Delta\theta \sim 0.2°$
- Mass $\Delta m/m \sim 1/160$

F. Cappuzzello et al., Eur. Phys. J. A (2016) 52: 167
M. Cavallaro et al., NIM B 463 (2020) 334

The multi-channel approach

There are **competing processes** leading to the **same final states** as **DCE**

Multi-channel approach: study under the **same experimental condition** the **complete net** of reaction channels that contribute to the DCE cross-section

F. Cappuzzello et al., Prog. Part. Nucl. Phys. 128 (2023) 10399

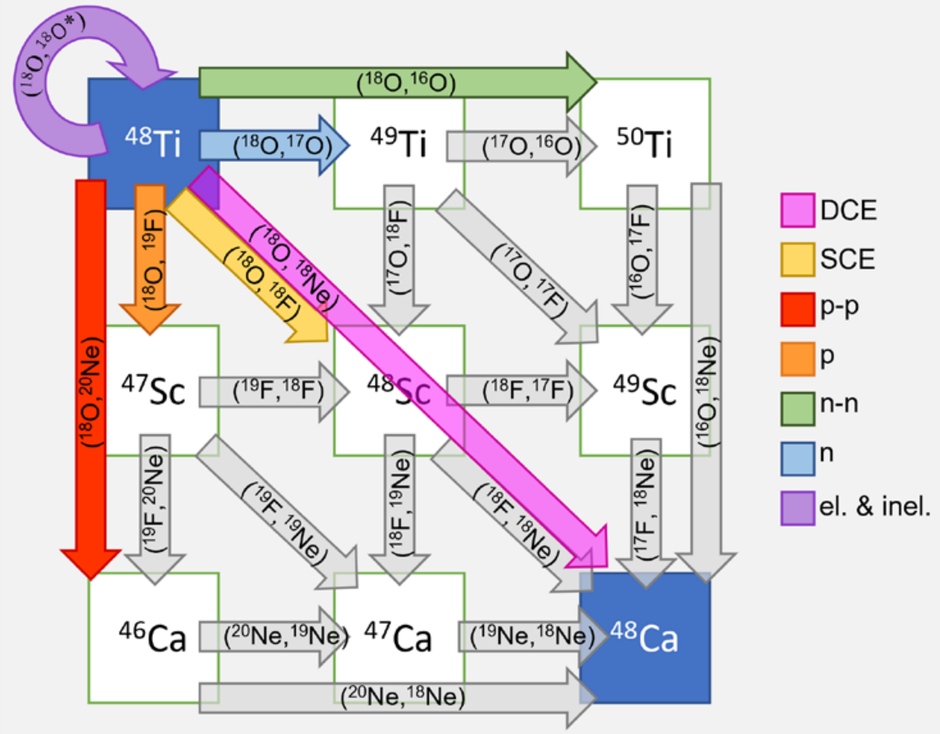

The multi-channel approach

There are **competing processes** leading to the **same final states** as **DCE**

Multi-channel approach: study under the **same experimental condition** the **complete net** of reaction channels that contribute to the DCE cross-section

F. Cappuzzello et al., Prog. Part. Nucl. Phys. 128 (2023) 10399

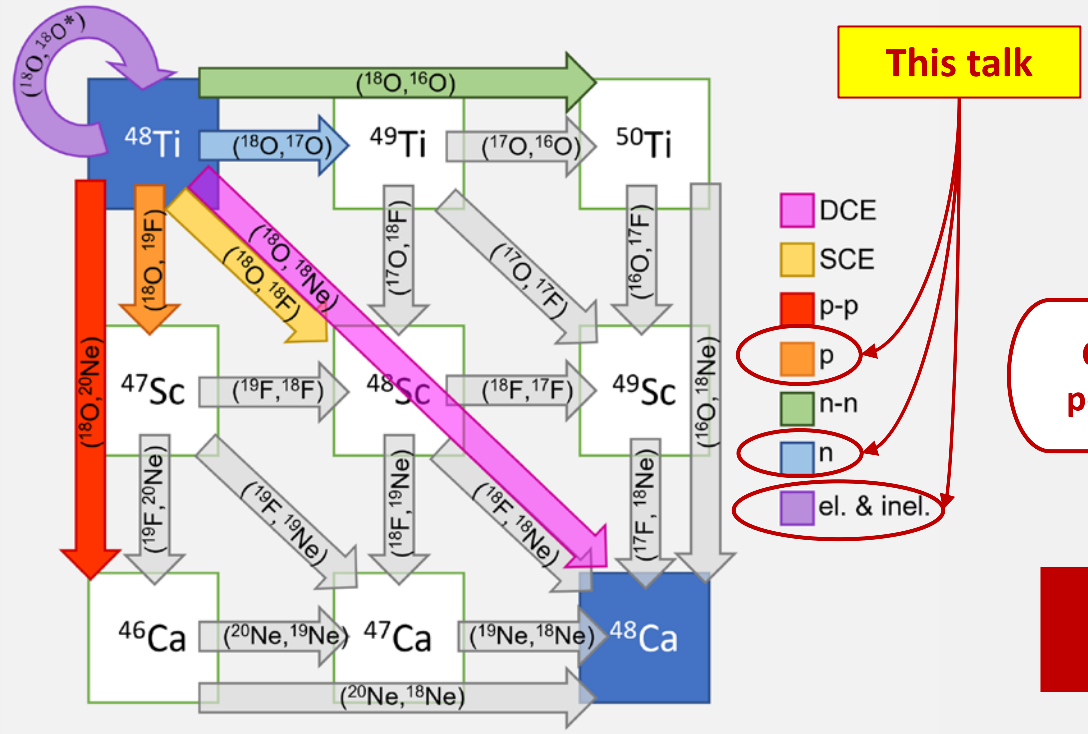

Why study elastic and inelastic scattering?

- **Optical potential**
- **Coupling effects**

→ **Initial State Interaction (ISI)**

Why study one-nucleon transfer?

- To evaluate the **contribution** of **multi-step nucleon transfer** to DCE cross-section
- To access **single-particle configurations** in nuclear states

The $^{18}O + ^{48}Ti$ experiment

MAGNEX magnetic spectrometer

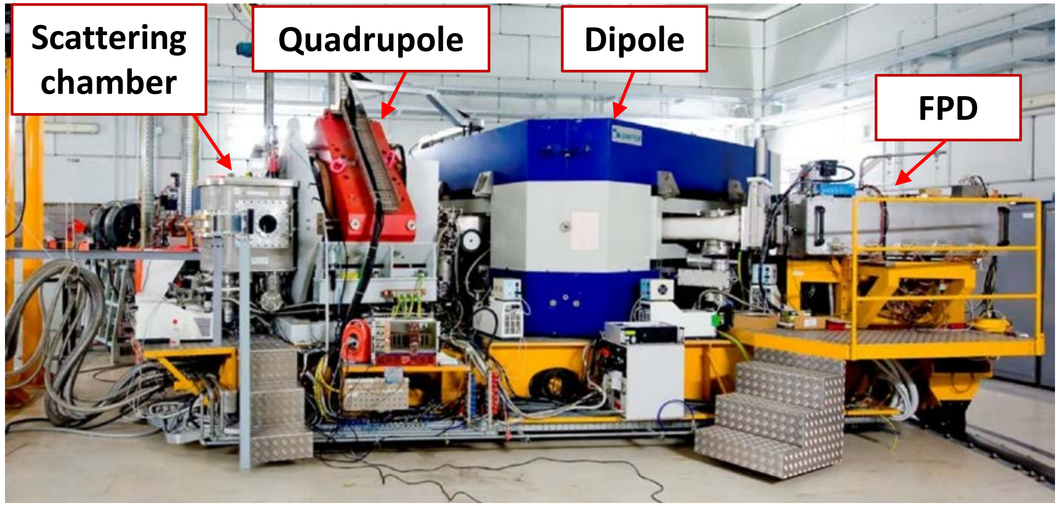

F. Cappuzzello et al., Eur. Phys. J. A 52 (2016) 167

Experimental set-up

- **Beam**: $^{18}O^{8+}$ at 275 MeV
- **Target**: TiO_2 evaporated onto Al
- **Optical axis**:
  - Elastic & inelastic: $\theta_{opt} = 9°, 15°$, and $21°$
  - 1-proton & 1-neutron transfer: $\theta_{opt} = 9°$

Focal Plane Detector

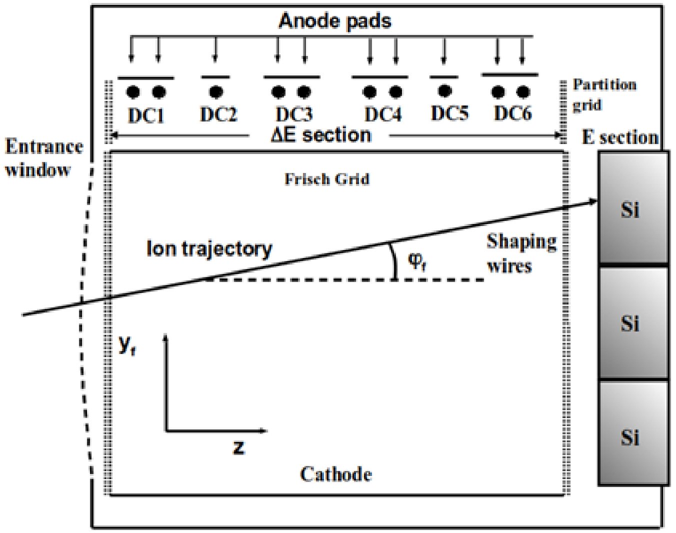

D. Torresi et al., NIM A 989 (2021) 164918

Hybrid detection system based on:

- **Proportional drift chamber:**
  - Measure of x, y, θ, φ
  - Measure of ΔE
- **Wall of 60 silicon detectors:**
  - Measure of E_{resid}

Particle Identification

F. Cappuzzello et al., Nucl. Instrum. Meth. A 621 (2010) 419

Elastic and inelastic scattering

G. A. Brischetto et al., Il Nuovo Cimento C 45 (2022) 96

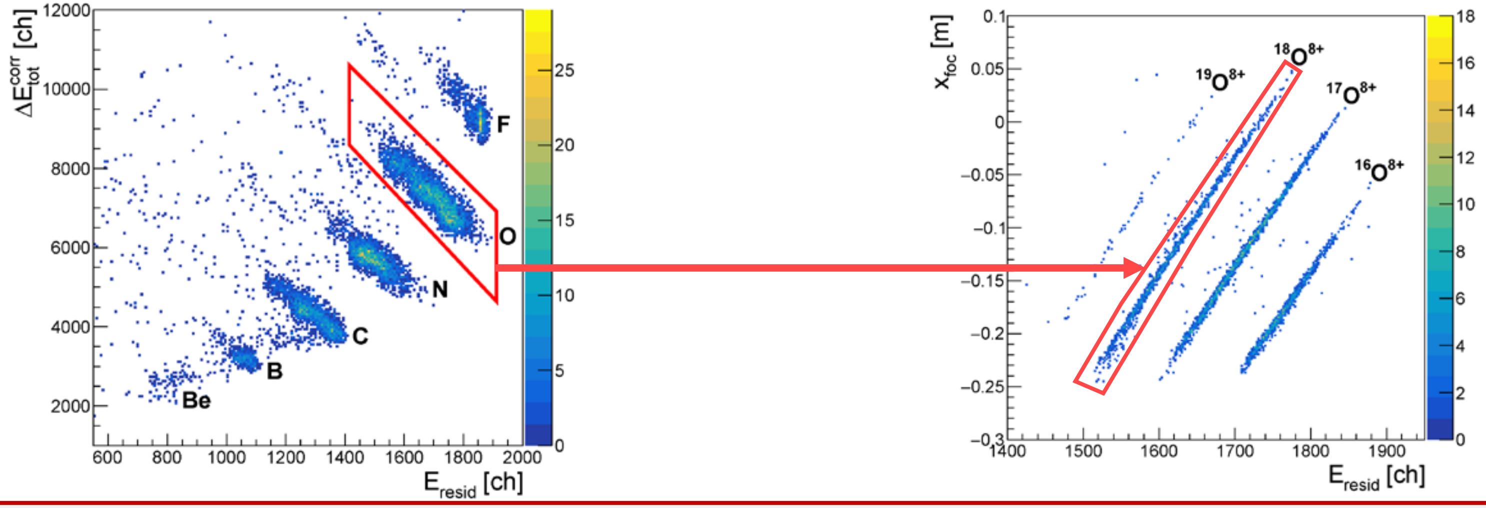

One-proton transfer channel $^{48}Ti(^{18}O,^{19}F)^{47}Sc$

O. Sgouros et al., Phys. Rev. C 104 (2021) 034617

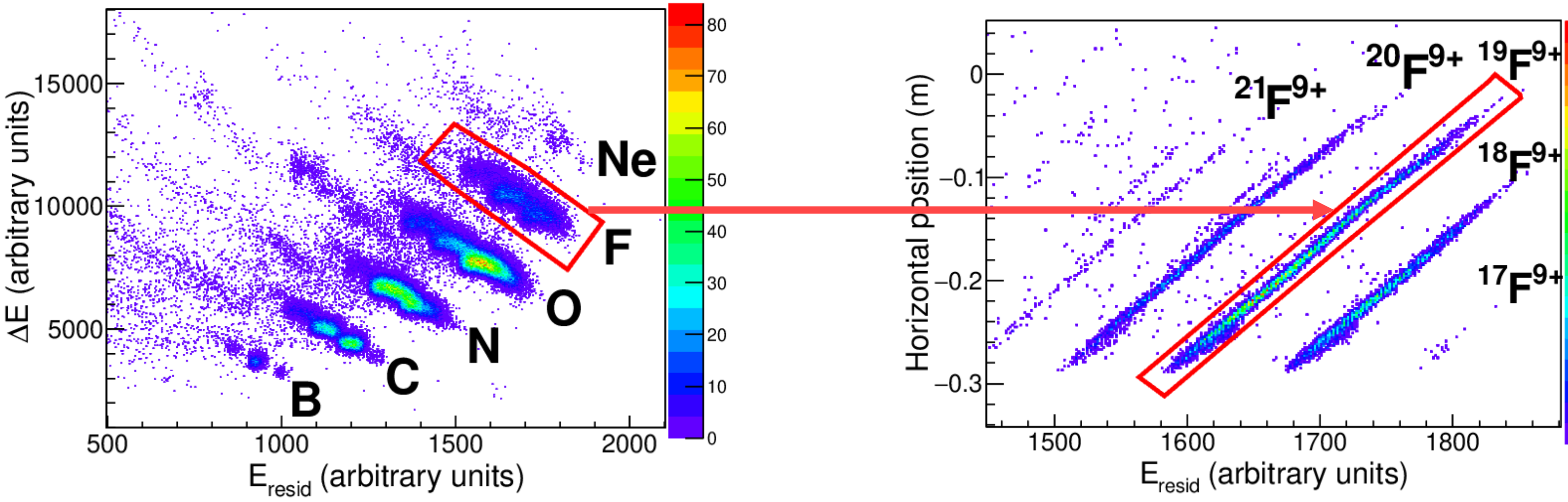

Elastic & inelastic scattering excitation energy spectrum

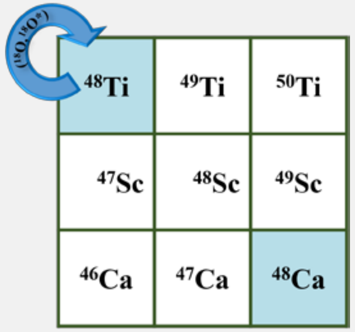

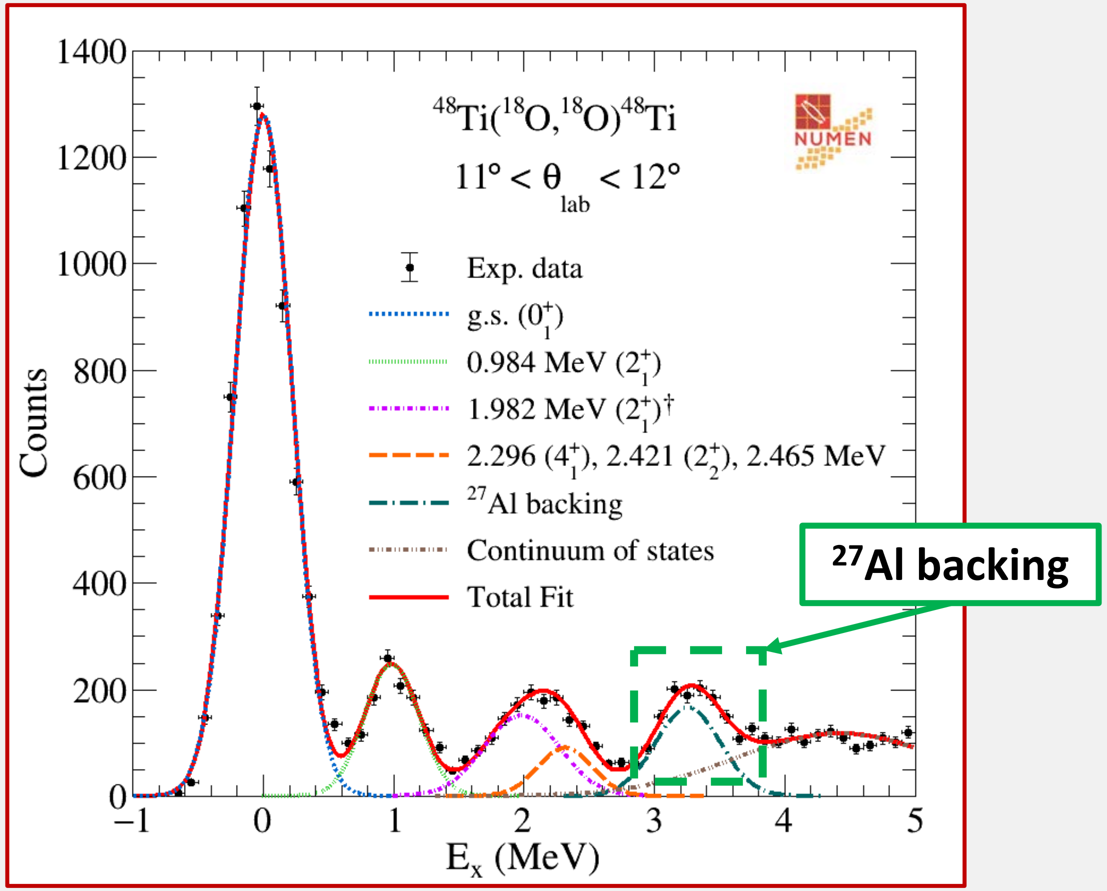

G. A. Brischetto et al., Phys. Rev. C 109 (2024) 014604

^{18}O		^{48}Ti	
E_x (MeV)	J^π	E_x (MeV)	J^π
0	0^+	0	0^+
1.982	2^+	0.984	2^+
3.555	4^+	2.296	4^+
3.634	0^+	2.241	2^+
3.920	2^+	2.465	
		2.997	0^+
		3.062	2^+
		3.224	3^+

Missing mass formula

$$E_x = Q_0 - K\left(1 + \frac{M_e}{M_r}\right) + E_{beam}\left(1 - \frac{M_b}{M_r}\right) + 2\frac{\sqrt{M_b M_e}}{M_e}\sqrt{E_{beam}K}\ \cos\theta_{lab}$$

Energy resolution ≈ 500 keV (FWHM)
Angular resolution ≈ 0.5°

Elastic & inelastic scattering theoretical analysis

Fully **quantum-mechanical theoretical calculations** performed within:

- **Optical Model** (OM)
- **Distorted wave Born approximation** (DWBA)
- **Coupled Channel** (CC)

Optical Potential:

- Double-folding **São Paulo Potential** V_{SPP}

$$U_{opt}(r) = (N_R + iN_I)\, V_{SPP}(r)$$

where

$$V_{SPP}(r) = e^{-\frac{4v^2}{c^2}} \int\int \mathrm{d}\mathbf{r}_1 \mathrm{d}\mathbf{r}_2\, \rho_1(\mathbf{r}_1)\, \rho_2(\mathbf{r}_2)\, V_{NN}(r_{12}, E_N)$$

L. C. Chamon et al., Phys. Rev. C 66 (2002) 014610

	N_R	N_I
OM/DWBA	1.0	0.78
CC	1.0	0.60

Elastic & inelastic scattering theoretical analysis

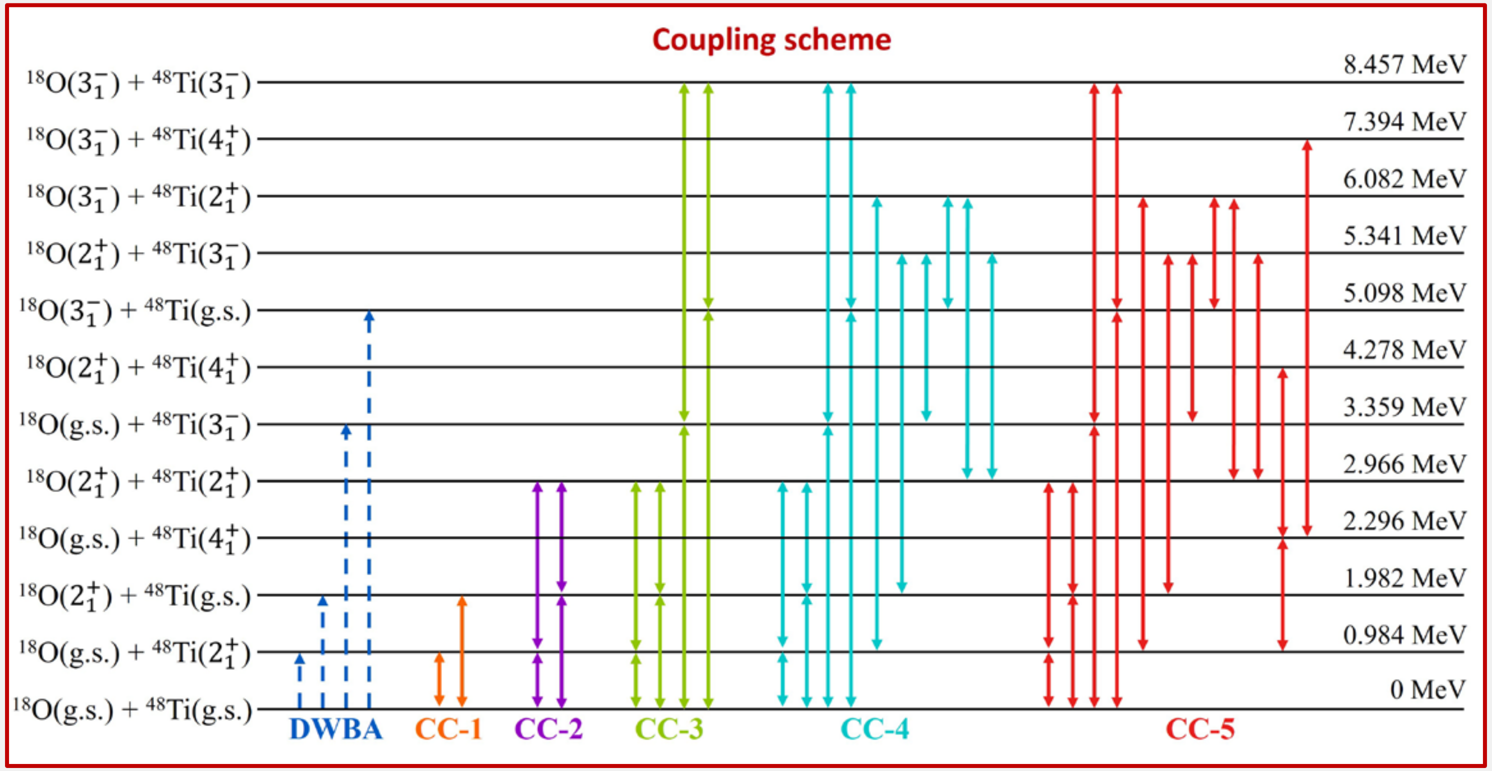

- **Rotational model** for the **2^+**, **3^-**, and **4^+** collective excited states of both **projectile** and **target**
- $\boldsymbol{M(E\lambda)}$ and $\boldsymbol{\delta_\lambda}$ from the literature

Coulomb coupling	$V_\lambda^{coul}(r) = \boldsymbol{M(E\lambda)}\, e^2 \frac{\sqrt{4\pi}}{2\lambda+1} \frac{1}{r^{\lambda+1}}$
Nuclear coupling	$V_\lambda^{nucl}(r) = -\frac{\boldsymbol{\delta_\lambda}}{\sqrt{4\pi}} \frac{dU_{opt}(r)}{dr}$

Elastic scattering cross-section angular distribution

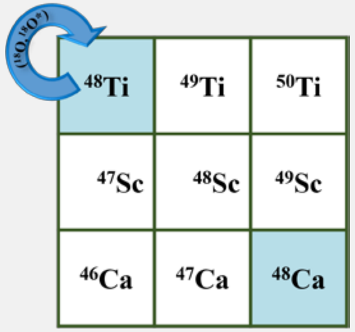

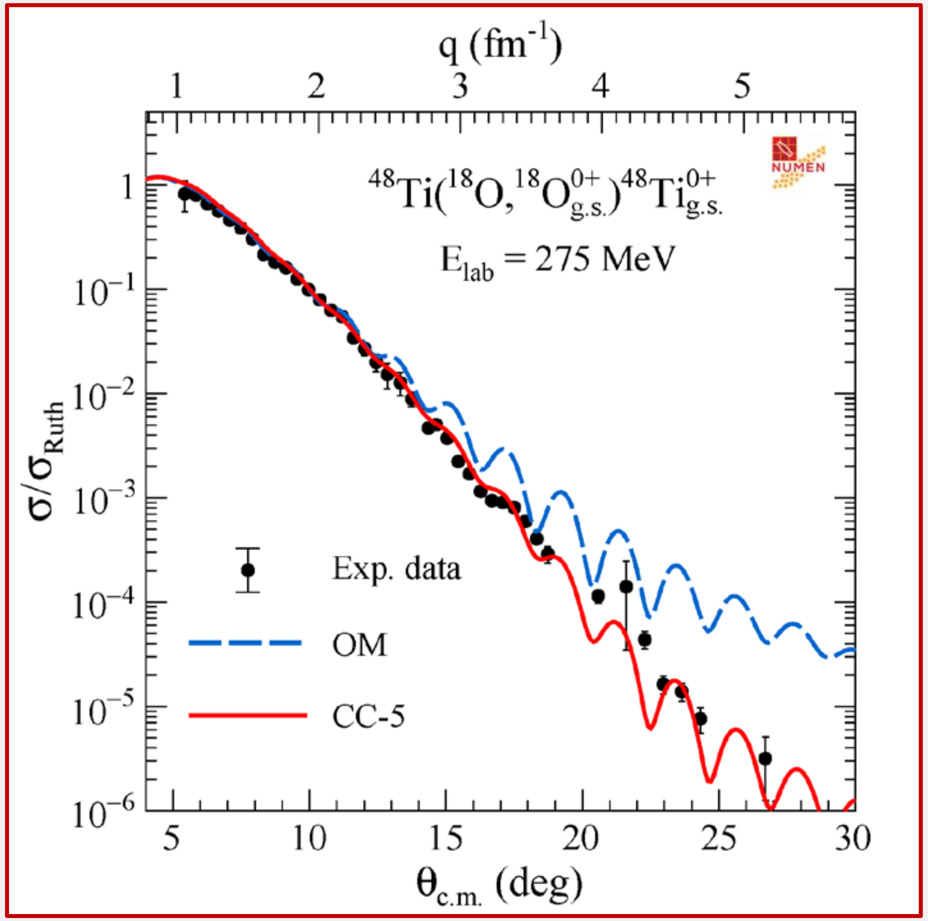

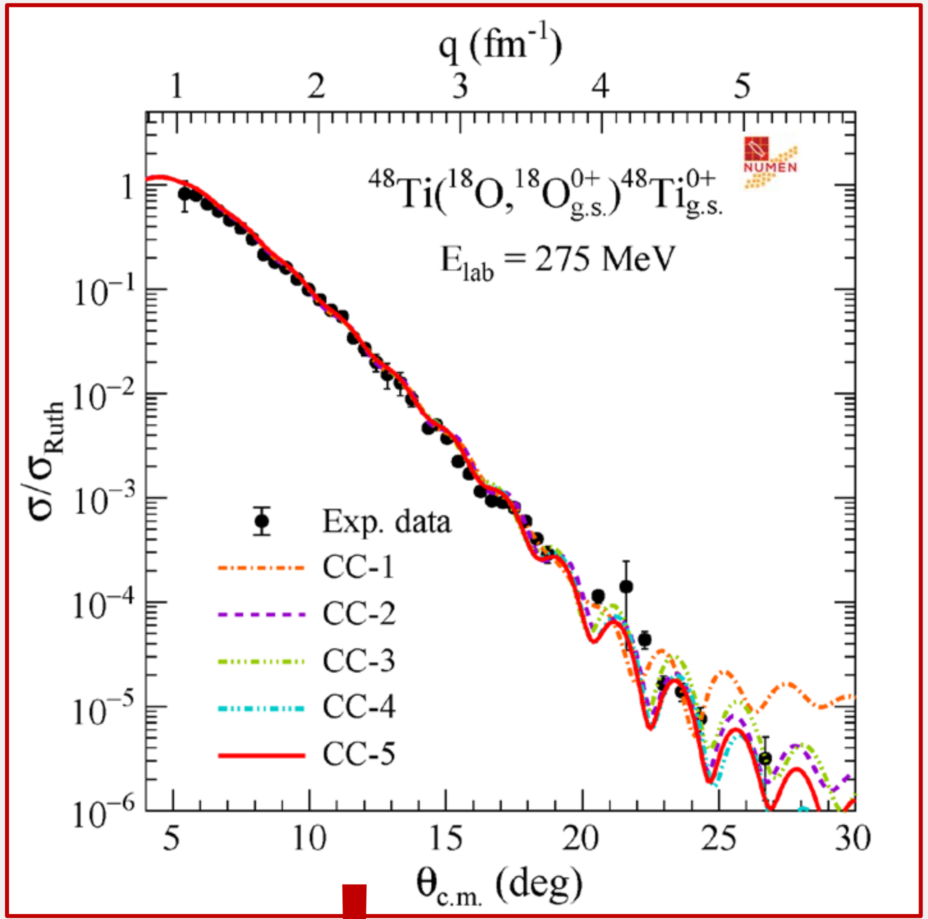

- **Optical model fails to reproduce the data at large momentum transfer**
- **Couplings to the low-lying collective states are relevant for a good description of the elastic scattering**

!

G. A. Brischetto et al., Phys. Rev. C 109 (2024) 014604

$^{48}\mathrm{Ti}(^{18}\mathrm{O}, ^{18}\mathrm{O}^{0+}_{g.s.})^{48}\mathrm{Ti}^{2+}_{0.984}$ inelastic scattering angular distributions

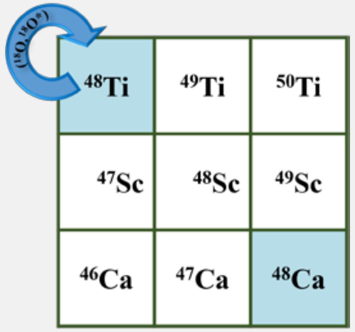

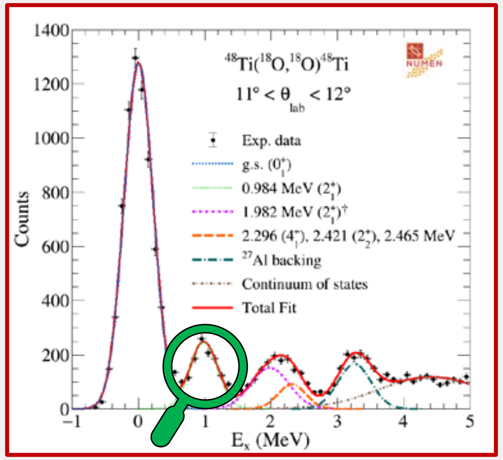

G. A. Brischetto et al., Phys. Rev. C 109 (2024) 014604

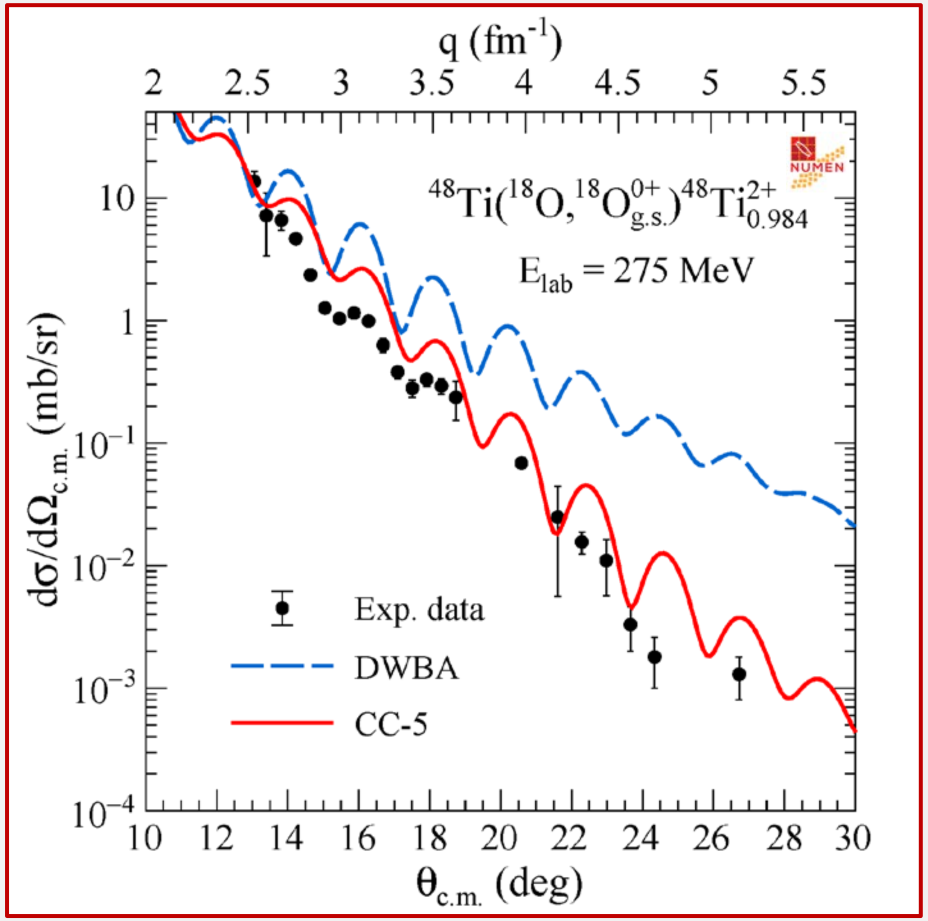

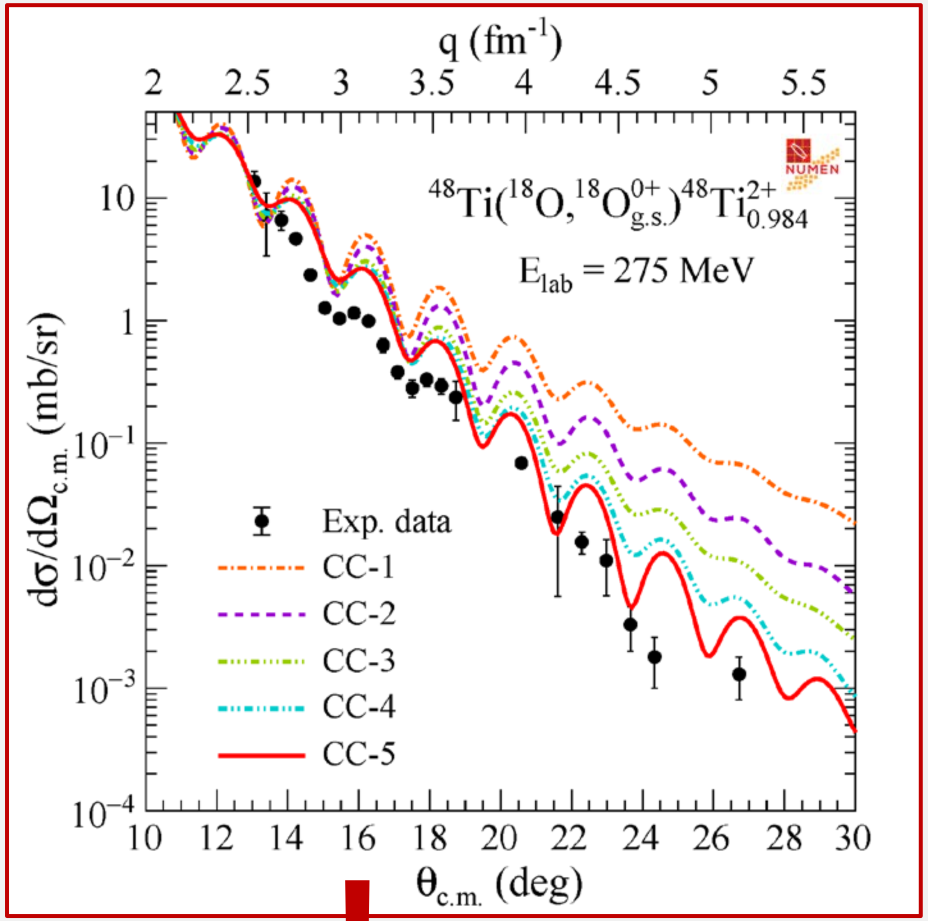

- **DWBA is not able to describe the experimental data**
- **Each enlargment of the coupling scheme produces a significant impact on the theoretical prediction**

Peak at 2.2 MeV inelastic scattering angular distributions

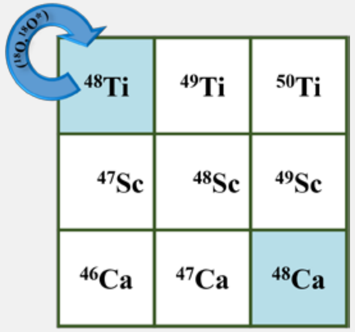

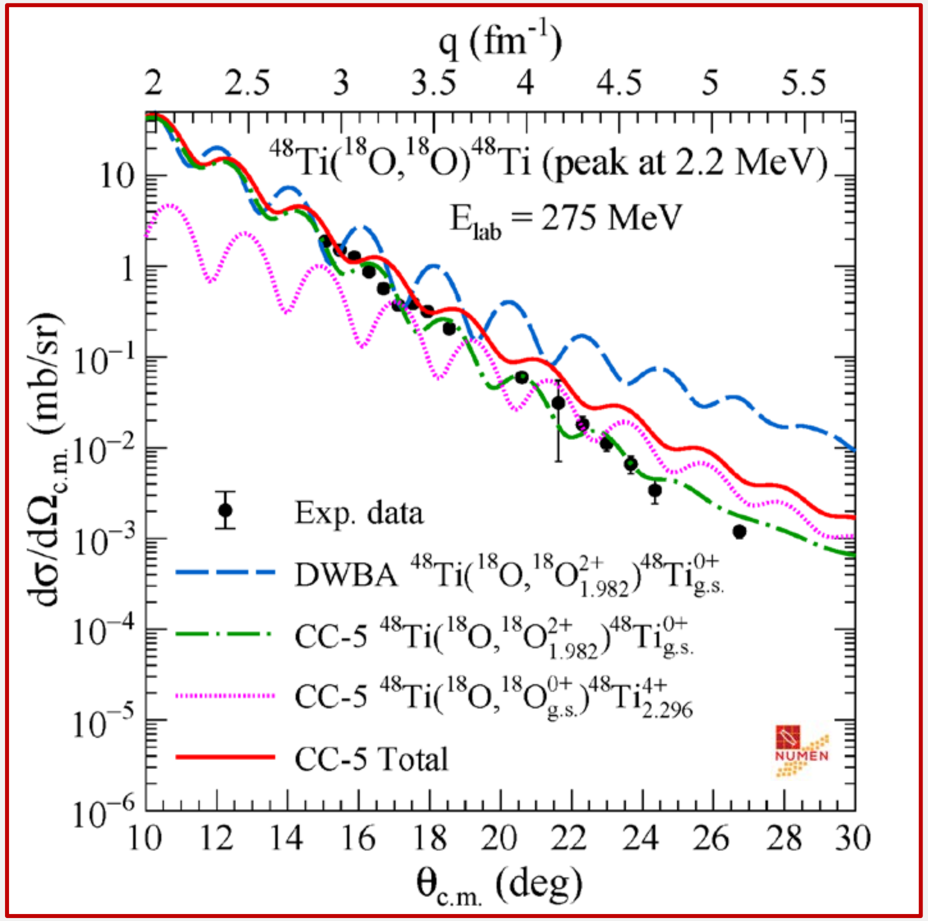

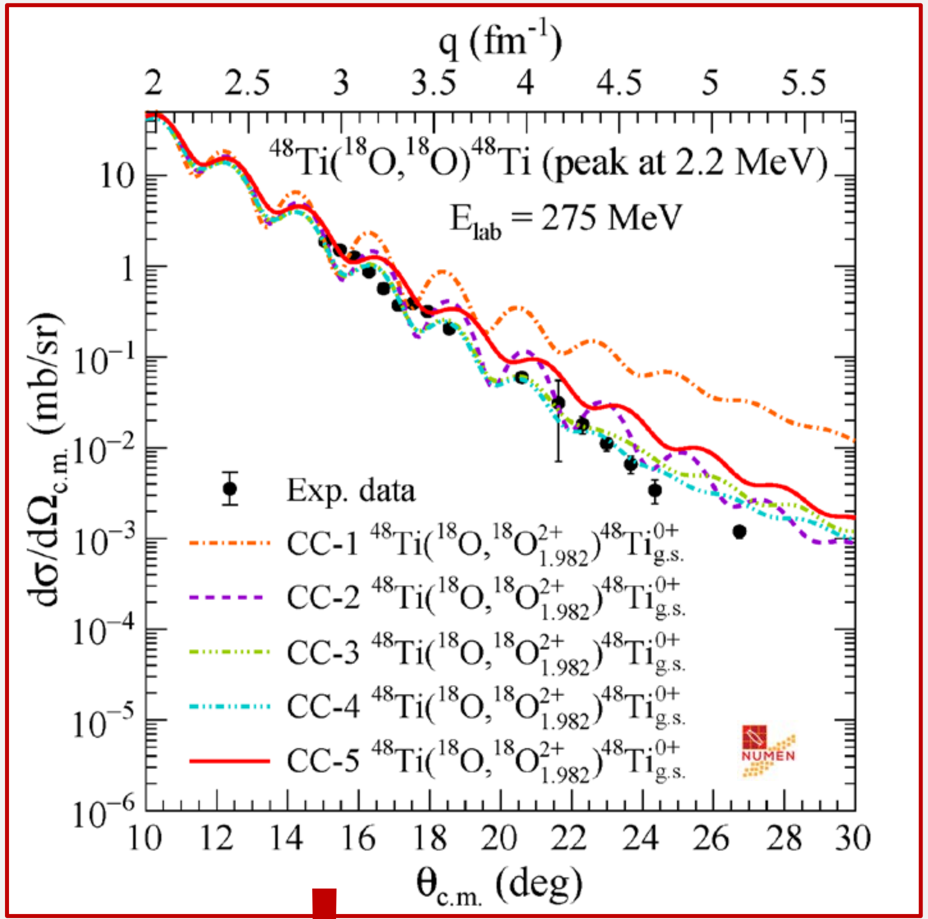

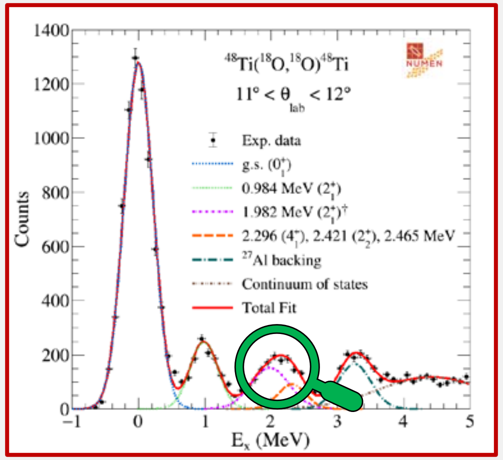

G. A. Brischetto et al., Phys. Rev. C 109 (2024) 014604

- **DWBA overestimates the experimental data**
- **Description of the data improved by using CC**

!

One-proton transfer reaction

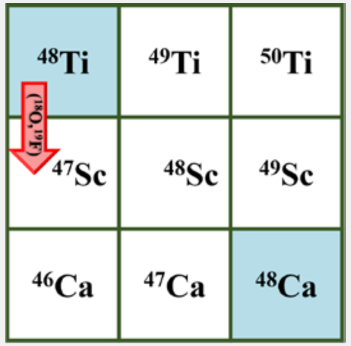

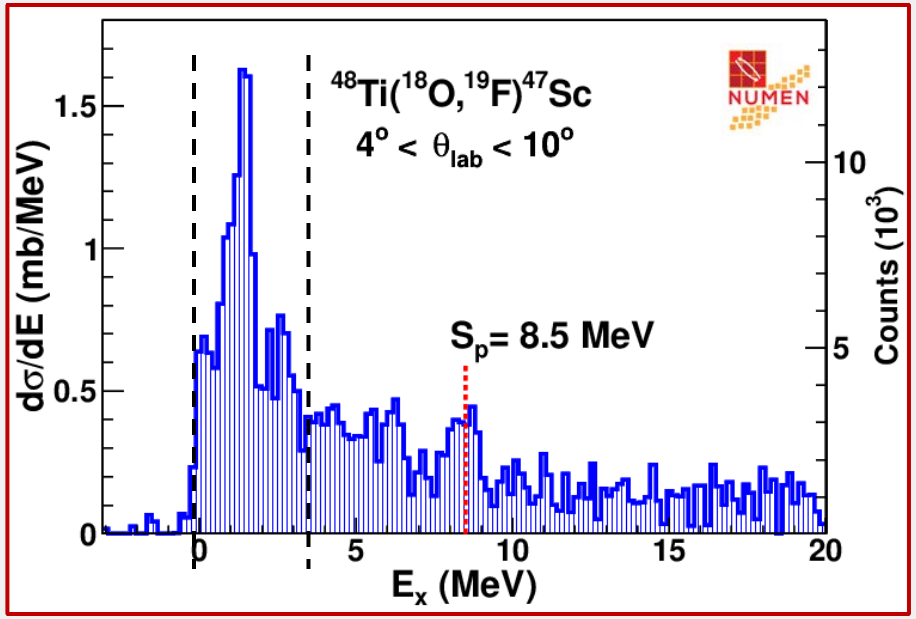

O. Sgouros et al., Phys. Rev. C 104 (2021) 034617

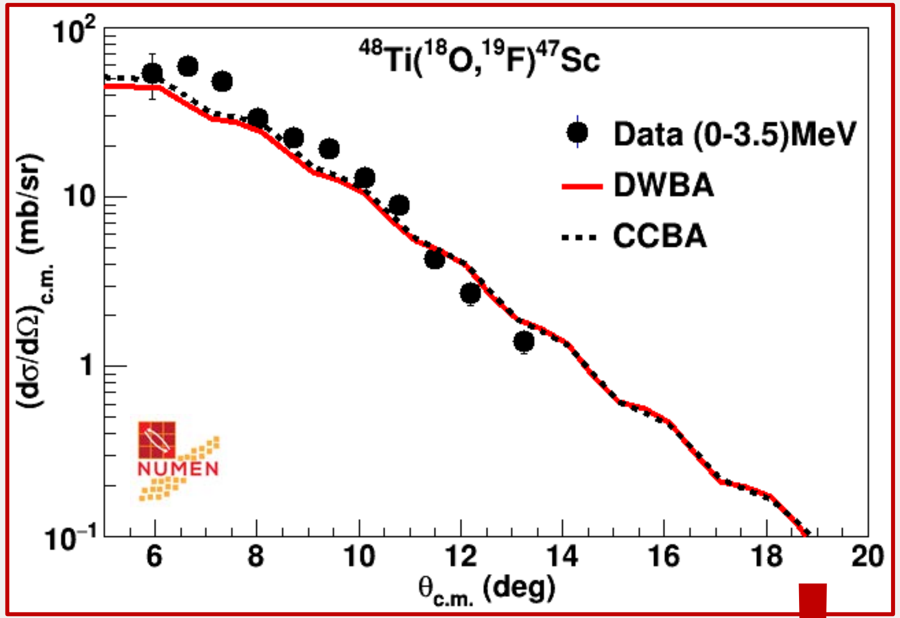

- **No significant role of core excitation**
- **Large-scale shell model calculations allow a reliable description of the data**

REACTION DYNAMICS → **Distorted waves: ISI** from the analysis of **elastic and inelastic scattering**

NUCLEAR STRUCTURE → **Spectroscopic amplitudes** derived from **large-scale shell model** calculations

Overlaps	Interaction	Core	Nucleon orbital
$<^{19}F\|^{18}O>$	P-SD-MOD	^{4}He	1p, 2s, 1d
$<^{47}Sc\|^{48}Ti>$	SDPF-MU	^{16}O	2s, 2d, 1f, 2p

One-neutron transfer reaction

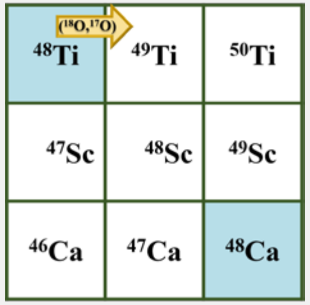

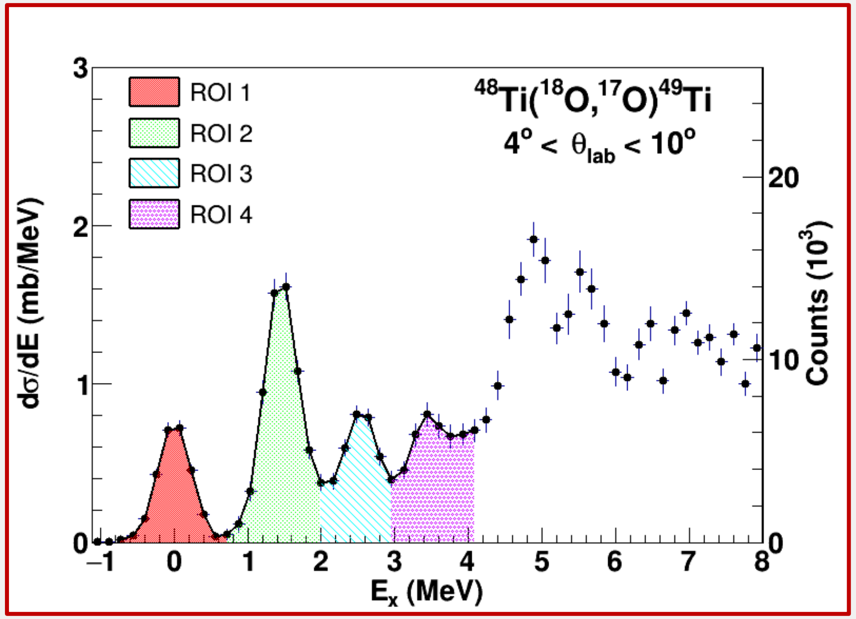

O. Sgouros et al., Phys. Rev. C 108 (2023) 044611

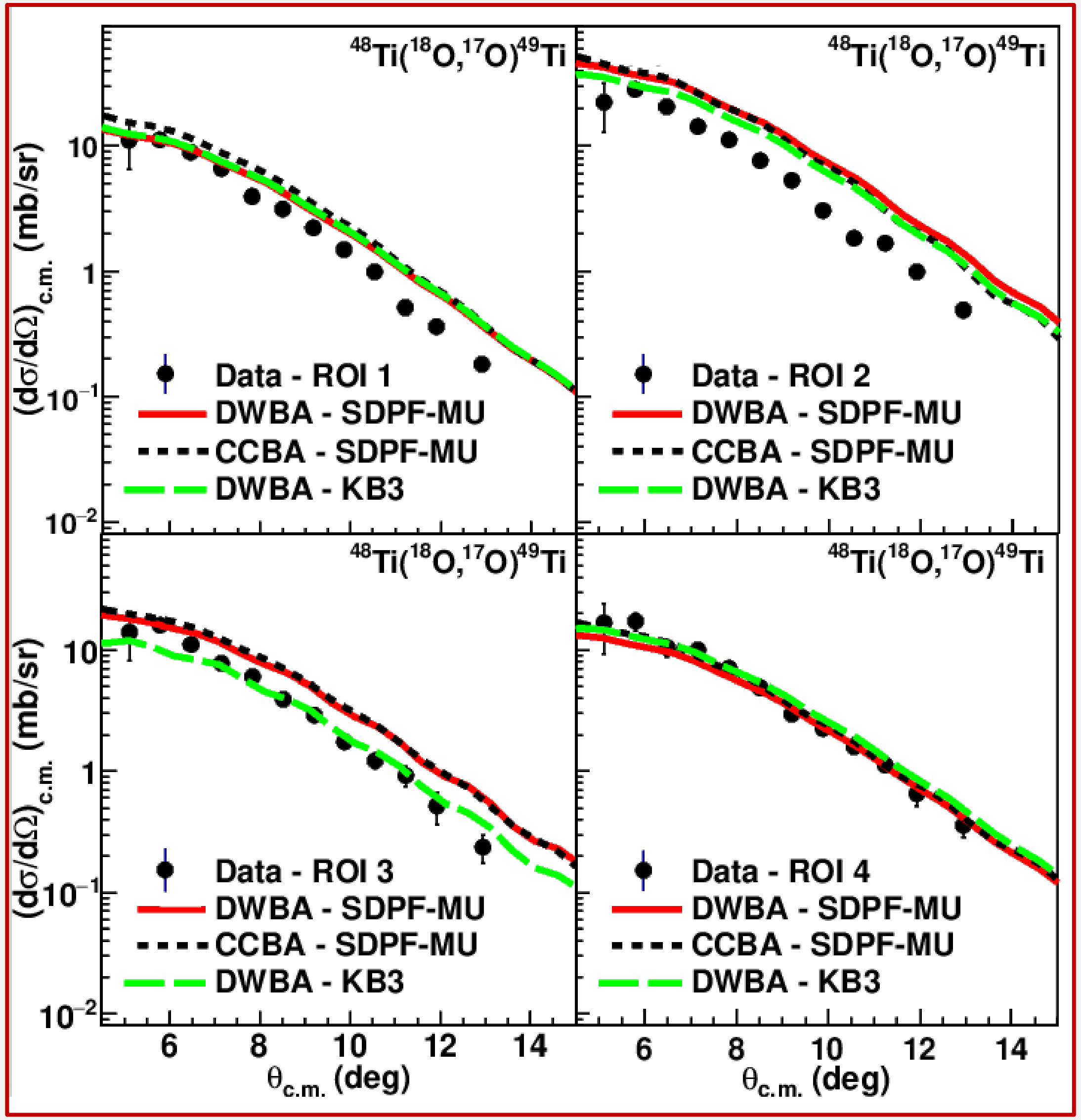

Same prescriptions as in one-proton transfer reaction

- **No significant role of core excitation**
- **Sensitivity to different effective interactions**

!

Overlaps	Interaction	Core	Nucleon orbital
<^{17}O|^{18}O>	P-SD-MOD	^{4}He	1p, 2s, 1d
<^{49}Ti|^{48}Ti>	SDPF-MU	^{16}O	2s, 2d, 1f, 2p
<^{49}Ti|^{48}Ti>	KB3	^{16}O	1f, 2p

Conclusion & Perspectives

- ✓ **Good agreement** between **experimental** and **theoretical** cross sections for elastic, inelastic and one-nucleon transfer channels **without any free parameter**
- ✓ **Couplings** to the low-lying collective states **relevant** for **ISI**, **not significant** for **one-nucleon transfer** reactions
- ✓ **Large-scale shell model** calculation provide good description of the data
- ✓ Sensitivity to different **effective interactions**

- o Completion of the analysis of the whole **^{18}O + ^{48}Ti reaction net**
- o Determination of the **DCE cross section** for the ^{18}O + ^{48}Ti system

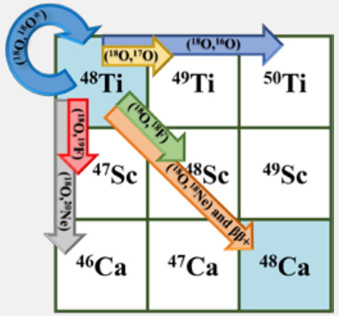

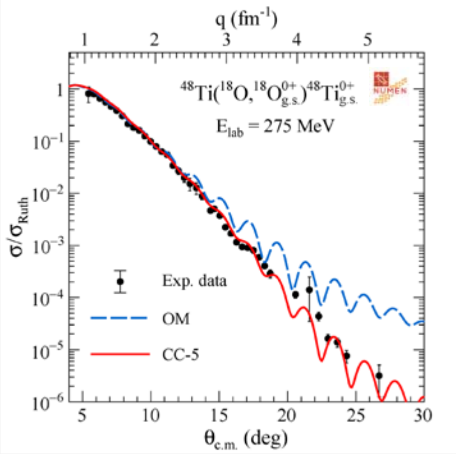

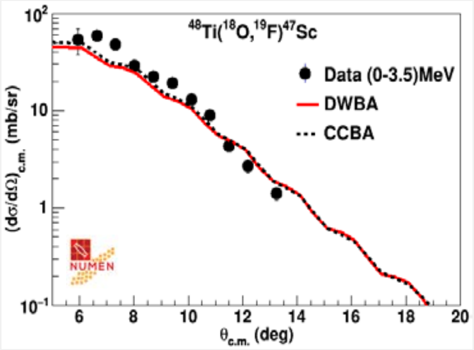

Thank you for your attention

Back up

Heavy-ion DCE reaction vs. 0νββ

Linear correlation between DCE DGT and 0νββ DGT and Total NMEs

Structure models adopted

- IBM formalism *E. Santopinto et al., PRC 98 (2018) 061601*
- Large scale shell model formalism *N. Shimizu, et al. PRL 120 (14) (2018) 142502*

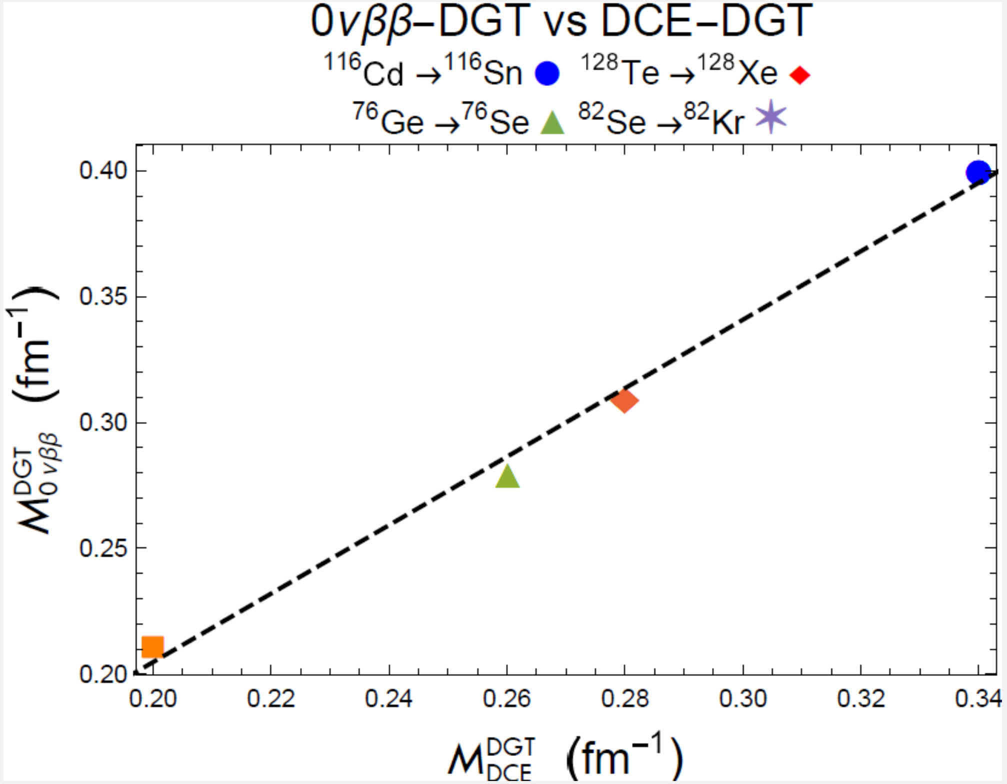

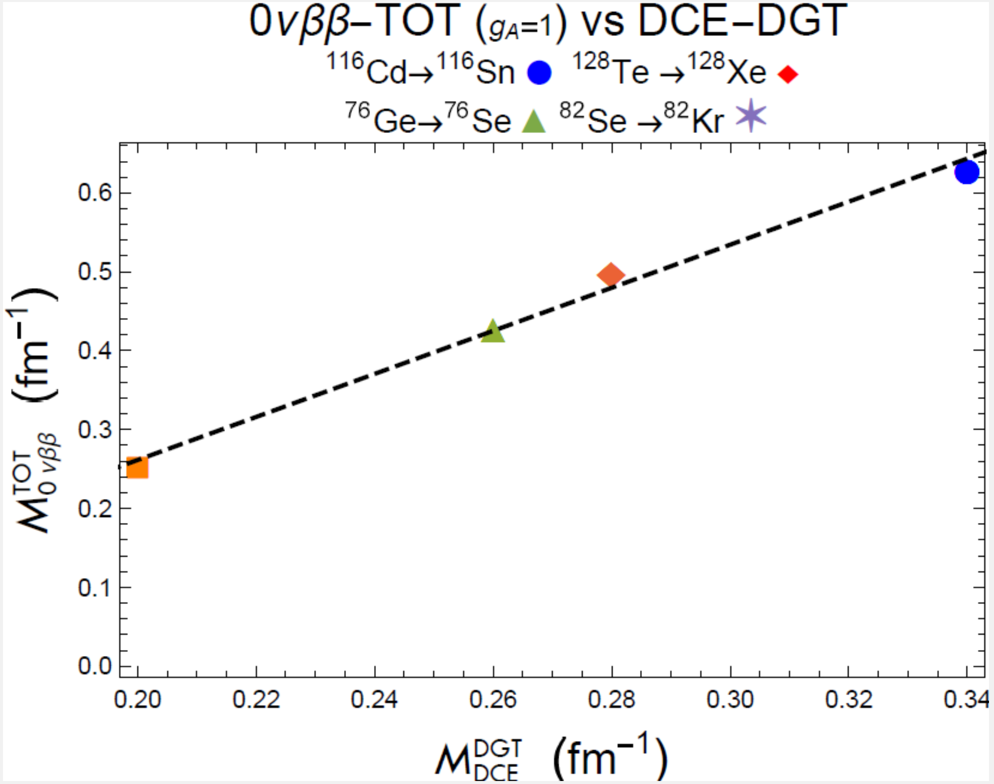

Application of the multi-channel approach

$^{40}Ca - {}^{40}Ar$

F. Cappuzzello et al. EPJ A 51, 145 (2015)
J.L. Ferreira et al., PRC 103, 054604 (2021)
M. Cavallaro et al., Front. Astron. Space Sci. 8, 659815 (2021)
S. Calabrese et al., PRC 104, 064609 (2021)

$^{116}Cd - {}^{116}Sn$

D. Carbone et al., PRC 102, 044606 (2020)
S. Calabrese et al., NIM A 980, 164500 (2020)
D. Carbone et al., Universe 07, 58 (2021)
S. Burrello et al. PRC 105, 024616 (2022)
J. Ferreira et al., PRC 105, 014630 (2022)

$^{76}Ge - {}^{76}Se$

A. Spatafora et al., PRC 100, 034620 (2019)
L. La Fauci et al., PRC 104, 054610 (2021)
I. Ciraldo et al., PRC 105 (2022) 044607
I. Ciraldo et al., PRC 109 (2024) 024615

$^{130}Te - {}^{130}Xe$

M. Cavallaro et al., Res. Phys. 13, 102191 (2019)
V. Soukeras et al., Res. Phys. 28, 104691 (2021)
D. Carbone et al., Universe 07, 58 (2021)

$^{48}Ca - {}^{48}Ti$

O. Sgouros et al., PRC 104, 034617 (2021)
O. Sgouros et al., PRC 108, 044611 (2023)
G. A. Brischetto et al., PRC 109, 014604 (2024)

$^{12}C - {}^{12}Be$

F. Cappuzzello et al., EPJ A 57, 34 (2021)
A. Spatafora et al., PRC 107, 024605 (2023)

Trajectory reconstruction

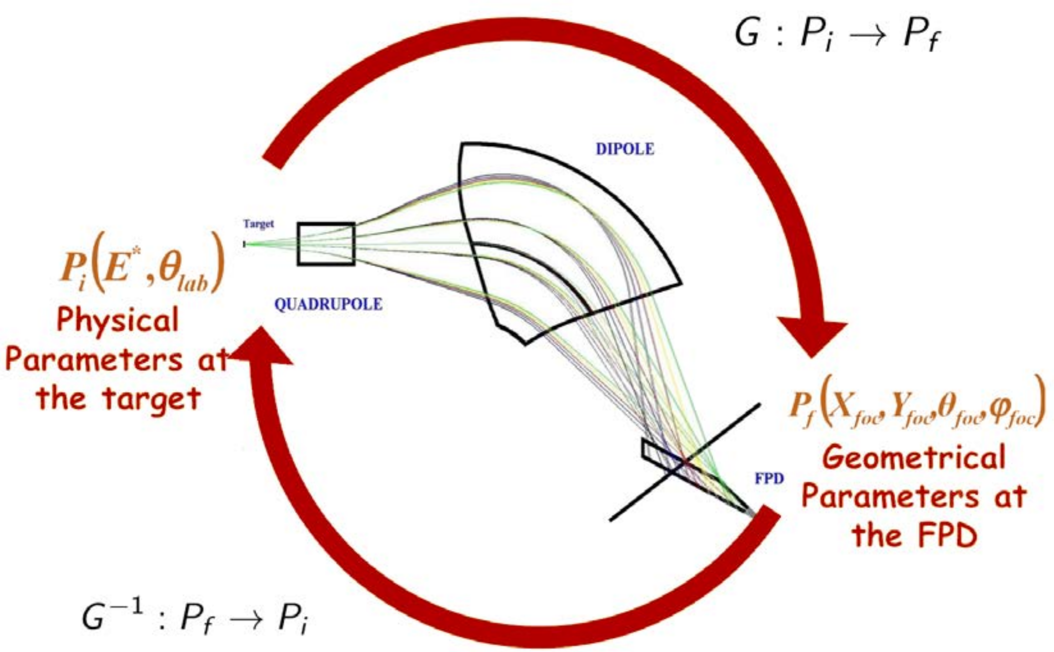

F. Cappuzzello et al., NIM A 638 (2011) 74

Measured parameters at the FPD

Trajectory Reconstruction
Need of solving the equation of motion up to the **10^{th} order**

COSY-INFINITY
K. Makino et al., NIM A 427 (1999) 338

Momentum vector at target position

Trajectory reconstruction

Elastic scattering

Data set 15deg

Final phase space parameters (measured)

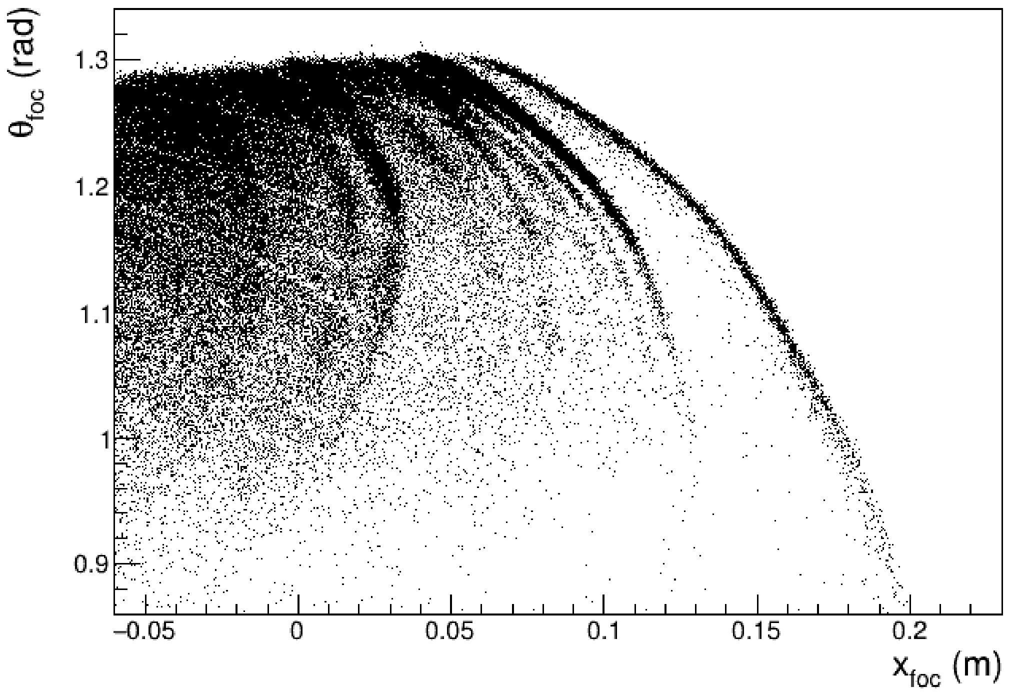

Initial phase space parameters

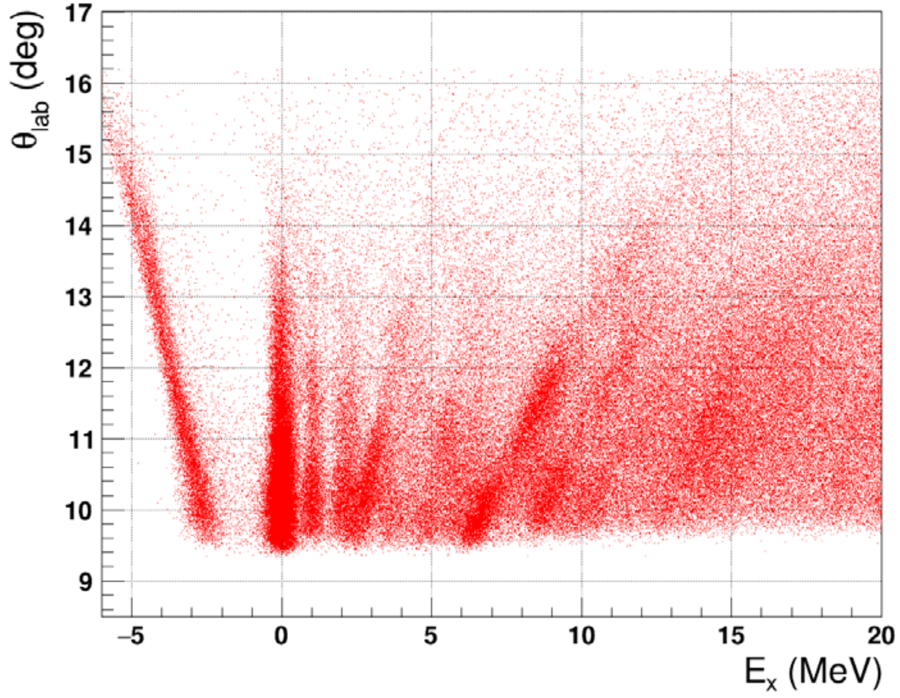

Inelastic scattering cross-section angular distributions

Coulomb coupling	$V_\lambda^{coul}(r) = M(E\lambda)\, e^2 \frac{\sqrt{4\pi}}{2\lambda+1} \frac{1}{r^{\lambda+1}}$
Nuclear coupling	$V_\lambda^{nucl}(r) = -\frac{\delta_\lambda}{\sqrt{4\pi}} \frac{dU_{opt}(r)}{dr}$

Theor. approach	N_W	J_V (MeV fm^3)	J_W (MeV fm^3)	σ_R (mb)
OM/DWBA	0.78	-346	-270	2571
CC	0.60	-346	-208	2498
CCEP	1.0	-258	-176	2480

$$R_V = \frac{\int dr\, 4\pi\, r^3\, V_{SPP}(r)}{\int dr\, 4\pi\, r^2\, V_{SPP}(r)}$$

	R_V (fm)	B(E2) (e^2 b^2)	M(E2) (e fm^2)	δ_2 (fm)	B(E3) (e^2 b^3)	M(E3) (e fm^3)	δ_3 (fm)
^{18}O	4.60	0.0043†	+6.56	0.75	0.0013§	+35.36	0.87
^{48}Ti		0.0720‡	+26.83	1.11	0.0074§	+86.02	0.77

†B. Pritychenko *et al.*, At. Data Nucl. Data Tables **107**, 1 (2016)

‡S. Raman *et al.*, At. Data Nucl. Data Tables **78**, 1 (2001)

§T. Kibédi and R. H. Spear, At. Data Nucl. Data Tables **80**, 35 (2002)

One-proton transfer background subtraction

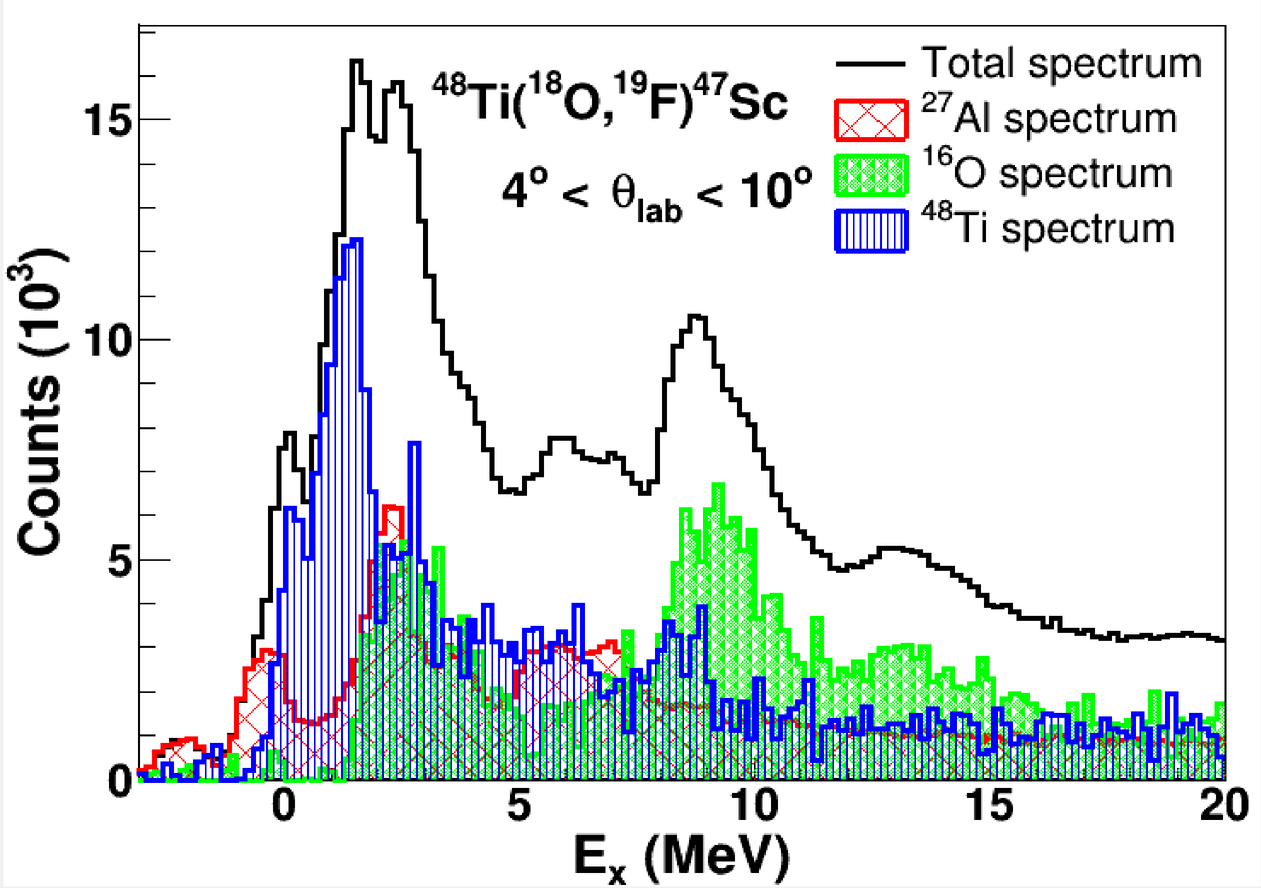

O. Sgouros et al.,
PRC 104 (2021) 034617

One-proton transfer DWBA ingredients

$$\frac{d\sigma}{d\Omega} \propto \left|T^{DWBA}\right|^2 = \left|\int d\vec{r}_\alpha d\vec{r}_\beta x_\beta^{(-)*} \langle \phi_B \phi_b \left| V \right| \phi_A \phi_a \rangle x_\alpha^{(+)} \right|^2$$

Distorted waves $\chi_{\alpha,\beta}$

- Describe the elastic scattering at the entrance(α) and exit(β) channels
- Solutions of Schrödinger equation adopting the **Optical Model**

Overlap functions

- $\varphi_{\ell sj}$ are single-particle solutions of a Woods-Saxon potential.
- Coefficients $A_{\ell sj}$ and $B_{\ell sj}$ are the spectroscopic amplitudes derived from shell-model calculations.

$$\langle \phi_B | \phi_A \rangle \propto A_{\ell sj} \varphi_{\ell sj}^{Bx}$$

$$\langle \phi_b | \phi_a \rangle \propto B_{\ell sj} \varphi_{\ell sj}^{ax}$$

Overlaps	Interaction	Core	Nucleon orbital
$<^{19}F\|^{18}O>$	P-SD-MOD	^4He	1p, 2s, 1d
$<^{47}Sc\|^{48}Ti>$	SDPF-MU	^{16}O	2s, 2d, 1f, 2p

One-proton transfer coupling scheme

Projectile Overlaps

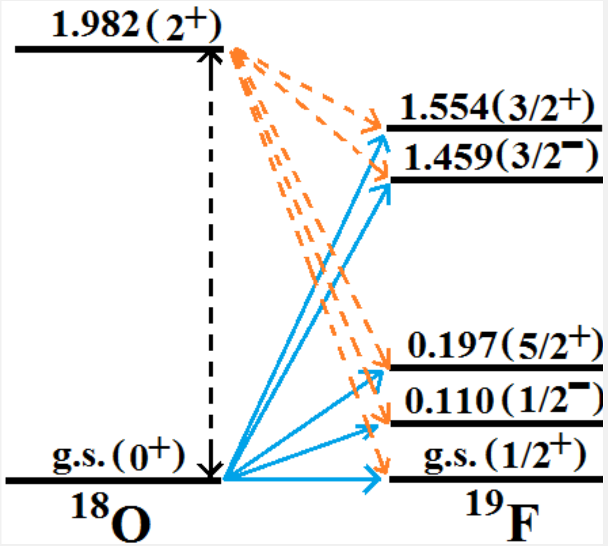

Target Overlaps

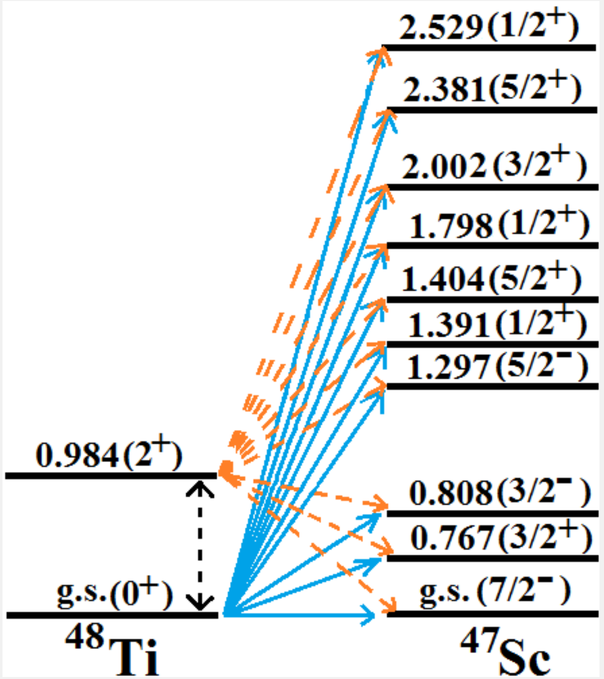

Blue arrows: DWBA calculation
Orange arrows: CCBA calculation